Predicting the X-ray Absorption Spectrum of Ozone with Single Configuration State Functions

Diptarka Hait[1] and Todd J. Martínez[1,2,*]

[1]Department of Chemistry and The PULSE Institute, Stanford University, Stanford, CA 94305

[2]SLAC National Accelerator Laboratory, 2575 Sand Hill Road, Menlo Park, CA 94025

*E-mail: todd.martinez@stanford.edu; toddjmartinez@gmail.com

Abstract

X-ray absorption spectra (XAS) of biradicaloid species are often thought to represent a challenge to theoretical methods. This has led to testing of recently developed multireference techniques on the XAS of ozone, but reproduction of the experimental spectral profile has proven difficult. We utilize a minimal model consisting of a single configuration state function (CSF) per excited state to model core-level excitations of ozone, with the orbitals of each CSF optimized using the restricted open-shell Kohn-Sham (ROKS) method. This protocol leads to semiquantitative agreement with experimental XAS. In fact, we find that low-lying core-hole excited states in biradicaloids can be approximated with single CSFs despite ground state multireference character. We also report that the 1s→ π^* and 1s→ σ^* transitions have quite distinct widths for O_3. This reveals the importance of sampling over a representative range of geometries from the vibrational ground state for properly assessing the accuracy of electronic structure methods against experiment, instead of the popular procedure of uniformly broadening stick spectra at the equilibrium geometry.

Introduction

X-ray radiation can excite core-level electrons into unoccupied levels, resulting in X-ray absorption spectra (XAS) that contain information about the local chemical environment around target atoms.[1] The strong element specificity and relative site specificity of XAS has contributed to its popularity for characterizing chemical systems.[1,2] In particular, time-resolved XAS (TR-XAS) has recently emerged as a powerful tool for pump-probe studies of chemical dynamics[3,4]. The increasing experimental interest in XAS has led to considerable recent efforts towards accurate computation of core-electron excitation energies and oscillator strengths, utilizing approaches like time-dependent density functional theory (TDDFT),[5,6] orbital-optimized density functional theory (OO-DFT),[7] algebraic diagrammatic construction (ADC)[8] and equation of motion coupled cluster (EOM-CC) theory,[9–11] among others.

These methods are however typically benchmarked against experimental results for the electronic ground state of closed-shell small molecules,[5,8,9,12] which are not necessarily representative of the transient species that may arise during photoinduced dynamics. For instance, homolytic bond fission in cyclic systems can lead to biradicaloid species[13–16] where the two highest energy electrons are neither completely paired (as in a perfectly closed-shell molecule) nor fully unpaired (as in two infinitely separated radical centers).[17] A qualitative description of the wavefunction of such molecules requires at least two Slater determinants.[18] Canonical examples of such biradicaloid species are highly reactive species like carbenes or benzynes, whose transient nature makes it difficult to unambiguously obtain experimental XAS.

The ozone (O_3) molecule is traditionally considered to have a biradicaloid electronic ground state,[20–22] with partial unpairing of the electrons in the formally highest occupied molecular orbital (HOMO, $1a_2$) into the lowest unoccupied molecular orbital (LUMO, $2b_1$). Full-valence complete-active space self-consistent field (CASSCF)[23] calculations indicate that the natural orbitals corresponding to the HOMO and LUMO (henceforth referred to as HONO and LUNO for simplicity, see Fig. 1) have occupations of 1.78 and 0.26, respectively (deviating significantly from the ideal closed-shell limit of 2 and 0). The biradicaloid character of O_3 can result in challenges for quantum chemical modeling. For example, CC through quadruple excitations is necessary to predict the total atomization energy of O_3 to the 'chemical accuracy' limit of 1 kcal/mol.[24] O_3 however is sufficiently stable to permit experimental XAS measurement[25,26] and therefore appears to offer a unique opportunity to assess multireference approaches for molecular XAS computation of biradicaloid systems.

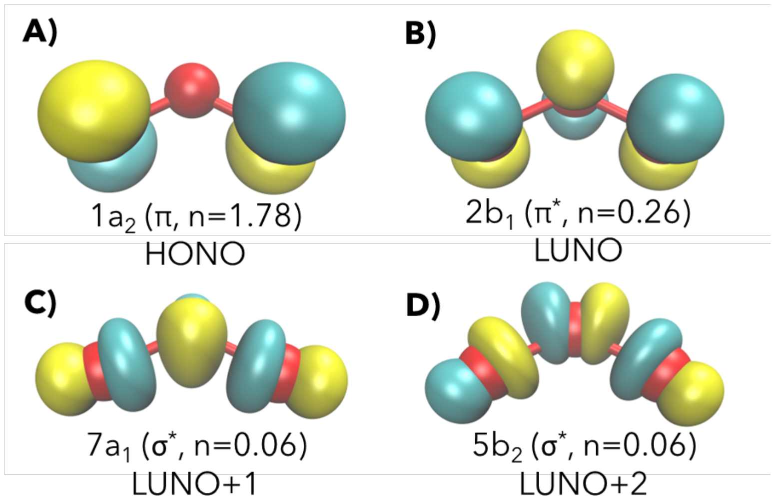

Figure 1: Frontier natural orbitals of O_3, from full-valence (18 electrons in 12 orbitals) CASSCF/cc-pVDZ.[19] The σ/π symmetry and occupation values (n) are also shown. Only the ground electronic state was considered for this CASSCF calculation.

O_3 therefore has been used to examine the performance of linear-response complete active space self-consistent field (LR-CASSCF),[27] multistate restricted active space second order perturbation theory (MS-RASPT2),[28] driven similarity renormalization group multireference perturbation theory (DSRG-MRPT),[29] and multireference ADC[30] in predicting XAS. Some of these studies[27,29,30] also noted the challenges of modeling the spectrum with related single reference methods like second order ADC or EOM-CC singles and doubles (EOM-CCSD).[31] Computed spectra in Refs 28-30 utilize uniform broadening of ‘stick’ spectra computed at the equilibrium geometry, thereby neglecting all nuclear quantum effects. However, this ‘single-geometry’ approach makes it quite difficult to properly gauge the relative accuracy of different methods via comparison with experiment, especially because bound and dissociative states have quite distinct intrinsic broadening.[32] Indeed, Ref 29 observed that “none of the theoretical computations satisfactorily reproduce the intensity profile of the ozone XAS spectrum", despite apparently acceptable performance in predicting excitation energies (after empirically shifting the first peak to align with experiment).

It would therefore be interesting to predict the XAS of O_3 with a semiclassical treatment of nuclear quantum effects, wherein the results from a large number of geometries sampled from the nuclear vibrational state would be summed over in order to account for intrinsic width. As a first attempt, computationally efficient single-reference protocols (like TDDFT or OO-DFT) could be utilized and their performance thereby better assessed for this prototypical biradicaloid. This would be more indicative of predictive accuracy for TR-XAS, as the associated chemical dynamics are generally modeled with *ab initio* molecular dynamics (AIMD) simulations (with potential inclusion of nonadiabatic effects with methods like surface hopping[33] or ab-initio multiple spawning[34]) starting from nuclear initial conditions sampled from vibrational Wigner[35] distributions.[36,37] The CASSCF HONO and LUNO occupations indicate that the largest Slater determinant to contribute to the O_3 ground state is by far the aufbau occupied, closed-shell configuration. Therefore spin-restricted Hartree-Fock[18] (RHF) or Kohn-Sham[38] (RKS) solutions are the simplest single-reference approximations to the ground state, while XAS can be subsequently modeled with linear-response methods like TDDFT or EOM-CCSD, or through state-specific OO-DFT methods.

The OO-DFT model for dipole-allowed core-level excited states of species with closed-shell ground states is the restricted open-shell KS (ROKS) approach,[12,39] which attempts to access singlet excited states with two unpaired electrons in a spin-pure manner within the KS formalism. A singly excited Slater determinant $|\Psi_i^a\rangle$ corresponding to an excitation out of orbital i to orbital a from a closed-shell reference $|\Psi\rangle$, has two unpaired electrons of different spins and is therefore not a spin-eigenstate. Indeed, with a spin-restricted set of orbitals, this open-shell determinant is exactly half singlet and half triplet. The minimal, spin-adapted wavefunction $\frac{1}{\sqrt{2}}\left(|\Psi_i^a\rangle + |\Psi_{\bar{i}}^{\bar{a}}\rangle\right)$ (where $|\Psi_{\bar{i}}^{\bar{a}}\rangle$ corresponds to the excitation of the other spin) is necessary to represent a pure singlet state with two unpaired electrons. ROKS models the energy E_S of this minimal, two determinant, configuration state function (CSF) by assuming that the energy of $|\Psi_i^a\rangle$ is precisely halfway[40] between E_S and the corresponding single determinant triplet state $|\Psi_{\bar{i}}^a\rangle$, and optimizes orbitals to extremize E_S. We note that the optimal excited state orbitals from ROKS are generally not identical to the ground state orbitals. Computation of transition properties like oscillator strengths therefore have to be carried out through a nonorthogonal configuration interaction formalism.[41] Further details about ROKS can be found elsewhere.[7,12,42]

Results and Discussion

Analysis of Computed XAS

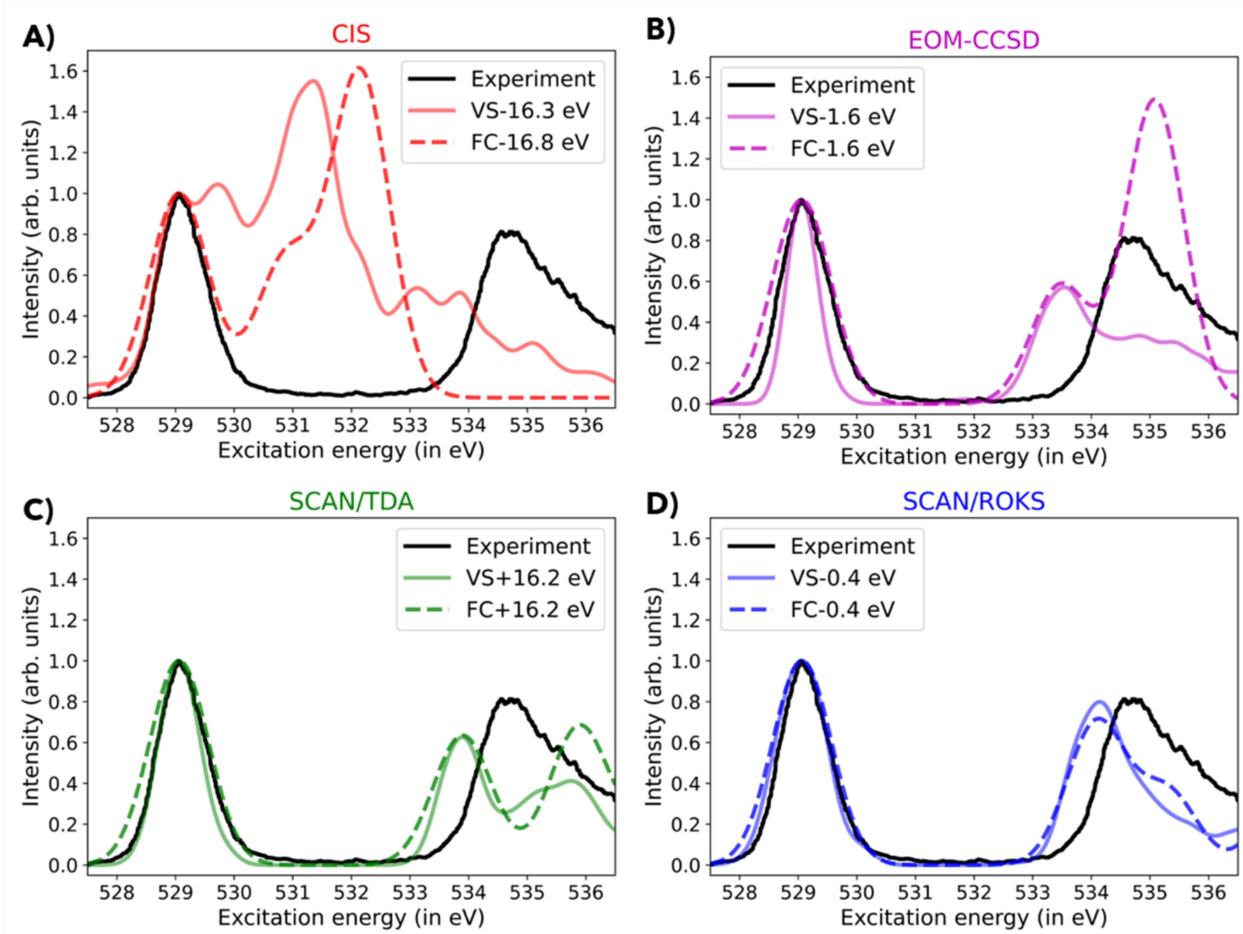

Figure 2: Computed XAS for O_3 from both geometries obtained from vibrational sampling (VS, solid colored line) and the single Franck-Condon (FC, dashed colored line) geometry with A) CIS, B) EOM-CCSD, C) TDDFT with SCAN and D) ROKS with SCAN, as compared to experiment[25] (black solid line). For VS, 128 geometries were sampled from the Wigner distribution corresponding to the vibrational ground state (within the harmonic approximation, utilizing the equilibrium geometry and normal modes computed from CCSD(T)/aug-cc-pVTZ). The computed peaks for each geometry were broadened by a Gaussian with $\sigma = 0.2$ eV and added together. Finally, the resulting spectrum is shifted (as indicated in the legend) to align the first local maximum with experiment. The computed peaks at the FC geometry were similarly broadened (with $\sigma = 0.5$ eV) and shifted to yield a single-geometry spectrum.

Fig. 2 compares the experimental XAS[25] with predictions from configuration interaction singles (CIS),[43] EOM-CCSD,[9] TDDFT within the Tamm-Dancoff Approximation (TDA[44]) with the SCAN[45] functional, and ROKS with SCAN. The SCAN functional was chosen on account of its good performance in predicting the XAS of closed-shell and monoradical molecules with OO-DFT[12,46] (spectra from some other functionals like PBE,[47] BLYP,[48,49] PBE0,[50] and B3LYP[51] are provided in the supporting information). Results from both a set of 128 geometries sampled from the vibrational wavefunction (VS) and the single Franck-Condon[52,53] geometry (FC) are presented. We focus only on the low energy regime of the spectrum, which has been previously interpreted[25] to arise from excitations out of the terminal oxygen (O_T) 1s orbitals to the $2b_1$ and $7a_1$ levels, as well as out of the central oxygen (O_C) 1s orbital to the $2b_1$. Specifically, the prominent peak at 529 eV in the experimental spectrum was assigned to $1s(O_T)\rightarrow 2b_1$, while the broad feature around 535 eV was attributed to both $1s(O_C)\rightarrow 2b_1$ and $1s(O_T)\rightarrow 7a_1$. These features will subsequently be referred to as the low- and high-energy peaks, respectively. The $1s(O_T)$ binding energy was determined to be 541.5 eV from experiment,[54] and a very large number of diffuse basis functions would therefore be necessary to properly describe the Rydberg states as this ionization edge is approached. This is computationally challenging, and is not attempted in this work. We note that analysis of practical TR-XAS measurements also tend to focus on the low energy region of the spectrum,[36,37,55,56] to avoid spectral congestion in the higher energy part where signal depletion from the parent molecule overlaps considerably with the new signal arising from products. We do however provide extensions of the O_3 K-edge spectra shown in Fig. 2 to higher energies (545 eV) in the supporting information, to show what can be achieved with these electronic structure methods and standard singly augmented basis sets[19,57–59] close to the K-edge ionization limit.

It is apparent that the CIS spectrum from either multiple geometries from vibrational sampling (VS) or the single FC geometry does not bear even a superficial resemblance to experiment (see Fig. 2A), indicating that CIS is not particularly suitable for modeling XAS of species with appreciable multireference character. The presence of correlation in the EOM-CCSD model leads to a better signal shape relative to experiment with the VS approach (see Fig. 2B), but the gap between the first two spectral maxima is appreciably underestimated (by $\sim$ 1 eV), as is the intensity of the high-energy peak. In addition, the higher energy feature predicted by EOM-CCSD with VS appears to be greatly broadened relative to experiment, and a third peak $\sim$ 535 eV can almost be discerned. The EOM-CCSD spectrum from the single FC geometry in fact shows three peaks, two corresponding to the first two VS spectral features and arising from excitations to the $2b_1$ level, as well as a very intense feature at $\sim$ 535 eV corresponding to the $1s(O_T)\rightarrow 7a_1$ transition. It thus appears that VS broadens the third peak considerably (thereby reducing peak height), indicating the different intrinsic widths of excitations to π^* and σ^* levels.[32] Nuclear quantum effects therefore cannot be neglected for proper modeling of the XAS of O_3 with EOM-CCSD (as well as related wavefunction methods).

TDDFT with the SCAN functional (see Fig. 2C) and the VS approach clearly bifurcates the higher energy spectral feature into two separate peaks, which is a behavior also observed for many other popular functionals (see supporting information). Interestingly, use of the FC geometry alone yields a relatively similar spectrum to VS and the $1s(O_T)\rightarrow 7a_1$ transition intensity is considerably smaller than what is predicted by EOM-CCSD. Comparison to other functionals (shown in the supporting information) shows that the $1s(O_T)\rightarrow 7a_1$ transition intensity with the FC approach increases significantly with the level of HF exchange present, though the significant broadening of this feature with VS leads to less variation in VS spectra across functionals. A superficial comparison of the VS and FC spectral profiles therefore indicates that VS is crucial for properly broadening the intense $1s(O_T)\rightarrow 7a_1$ feature for hybrid functionals, while being somewhat less so for local functionals. Overall, neither EOM-CCSD nor TDDFT yields computed spectra in good qualitative agreement with experiment, despite substantial empirical shifting to align the first peak. The high energy feature in experimental spectrum is predicted to be two separate peaks from both FC and VS, with the latter protocol broadening the third computed peak to a greater extent but not quite reproducing the experimental profile of a single peak with an asymmetric skew towards higher energies.

In contrast, ROKS/SCAN with the VS approach yields a spectrum in reasonable qualitative agreement with experiment (see Fig. 2D). A 0.4 eV redshift is necessary to align the low-energy peak with experiment,[25] which is comparable to the 0.3 eV root-mean-square error associated with this approach for small closed-shell molecules.[12] In this regard, it is worth noting that Refs 25 and 26 report experimental low-energy peak positions that differ by 0.2 eV. More interestingly, the intensity of the higher energy feature and its position are predicted to a greater accuracy than EOM-CCSD, despite the lower computational scaling of ROKS. The error in the high-energy peak position in the shifted spectrum vs experiment is 0.4 eV (but is ~ 0.0 eV if the unshifted computed spectrum is considered instead), indicating a better separation between the peaks than EOM-CCSD. More importantly, this feature is predicted to be a single peak with a skew towards higher energies from the VS approach, in agreement with experiment. ROKS/SCAN with VS therefore yields a semiquantitative description of the experimental O_3 XAS profile. The single geometry FC approach with ROKS also yields a relatively similar spectrum, though the $1s(O_T)\rightarrow 7a_1$ transition is visible as a distinct shoulder instead of the asymmetric skew observed in experiment and predicted by VS. At least to our perception, the level of agreement surpasses what was achieved with uniform broadening at a single geometry in prior studies utilizing explicitly multireference methods.[28–30] We also find that the PBE, BLYP, PBE0 and B3LYP functionals yield similar quality spectra with ROKS, albeit with some minor differences in peak positions (as shown in the supporting information). This indicates that the good performance of ROKS/SCAN was not fortuitous and reasonable results can likely be expected of other well-behaved density functional approximations.

Characterizing the Higher Energy Peak

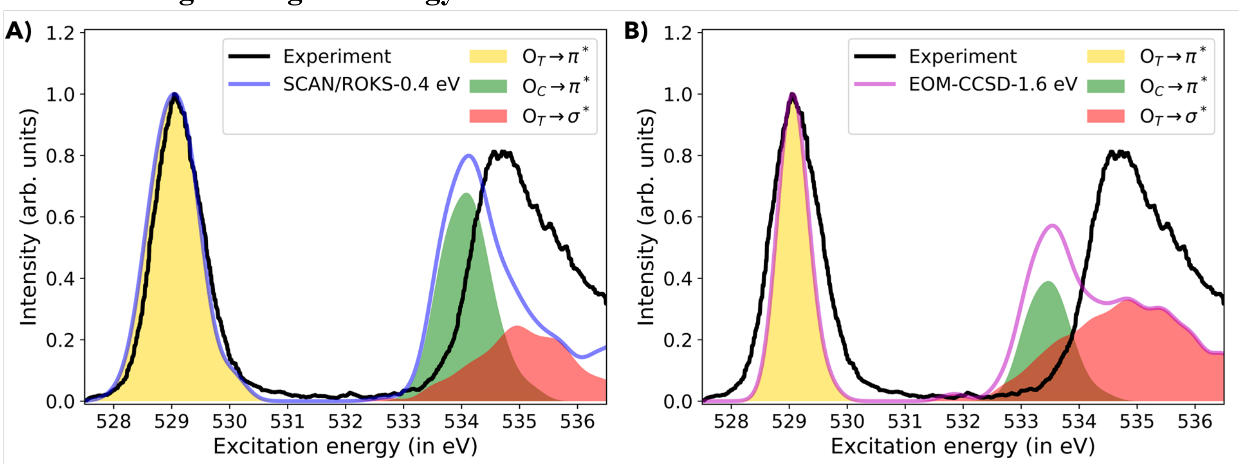

Figure 3: Decomposition of the computed XAS into $1s(O_{C/T})\rightarrow \pi^*/\sigma^*$ contributions (O_C refers to central oxygen atom, O_T to the terminal atoms) for VS spectra from A) ROKS with SCAN and B) EOM-CCSD.

The reasonable agreement between experiment and ROKS/SCAN with the VS approach leads us to deconvolute the relative contributions from the $1s(O_C)$ and $1s(O_T)$ levels in the high-energy peak. Spatial symmetry breaking in the distorted geometries sampled for VS and core-hole localization makes the precise C_{2v} symmetry orbital designations like $2b_1$ and $7a_1$ somewhat questionable. We therefore use π^* and σ^* labels instead (see Fig. 1), as triatomic O_3 must remain planar. The decomposition of the computed XAS into 1s($O_{C/T}$)→ π^*/σ^* contributions is depicted in Fig. 3 for both ROKS/SCAN and EOM-CCSD. The ROKS/SCAN VS spectrum indicates that the high energy peak maximum mostly arises from the relatively spectrally narrow 1s(O_C)→ π^*transition, while the much broader 1s(O_T)→ σ^* feature mostly contributes to the higher energy tail. This is consistent with experimental results using polarized radiation.[26]

Method	1s(O_T)→ π^*		1s(O_C)→ π^*		1s(O_T)→ $\boldsymbol{\sigma}^*$	
	E	f	E	f	E	f
Experiment*	529.0		+5.6		+6.5	
ROKS/SCAN	529.4	0.065	+5.0	0.045	+6.2	0.026
EOM-CCSD (Q-Chem)	530.6	0.088	+4.5	0.051	+6.1	0.130
EOM-CCSD (eT)	531.9	0.081	+4.4	0.047	+6.0	0.123
EOM-CC3 (eT)	529.9	0.070	+5.5	0.039	+6.2	0.054
MS-RASPT2[28]	529.0	0.074	+6.8	0.031	+7.5	0.067
MR-ADC(2)-X[30]	527.6	0.069	+5.5	0.030	+6.2	0.081
DSRG-MRPT3[29]	530.2	0.077	+5.1	0.033	+6.6	

Table 1: Comparison of computed excitation energies (E, in eV) and oscillator strengths (f) at the equilibrium geometry with ROKS/SCAN, EOM-CCSD, EOM-CC3, and prior work. The absolute 1s(O_T)→ π^*peak energy is reported, followed by spacings between this and other features. Experimental estimates for the band-maxima are also provided as a rough guide (the 1s(O_T)→ π^*peak energy value is obtained from digitizing the spectrum in Ref 25 and is then combined with the peak separations reported in Ref 26). No DSRG-MRPT3 oscillator strengths for the 1s(O_T)→ σ^* were reported in Ref 29. All calculations use slightly different parameters (geometries, basis sets, relativistic effects etc.) and comparisons therefore should only be treated as indicative guides. For instance, Q-Chem[50] and eT[51] utilize slightly different approaches for freezing cores for EOM-CCSD core-level calculations (see the Computational Methods section), leading to different numbers for the 1s(O_T)→ π^* peak energy but very similar peak spacings.

EOM-CCSD yields a qualitatively similar picture, except for the relative intensities. EOM-CCSD finds the 1s(O_C)→ π^* feature to be less intense than what is predicted by ROKS/SCAN, while the 1s(O_T)→ σ^* peak appears to be more intense (consistent with what can be seen from comparing VS to the corresponding FC geometry results in Fig. 2). EOM-CC3[11,62] calculations at the FC geometry indicate that the intensity of 1s(O_T)→ σ^* excitation is indeed likely being significantly overestimated by EOM-CCSD (see Table 1). Both ROKS/SCAN and EOM-CCSD VS spectra however clearly reveal that the intrinsic width of transitions to 1s→ π^* and 1s→ σ^* levels are quite distinct, with the latter being broader by a factor of ~ 2. Uniformly broadened spectra from the equilibrium geometry alone therefore appear to be quite insufficient to model XAS for species where transitions to both π^* and σ^* levels are relevant. It also potentially calls for re-evaluation of the performance of multireference approaches for modeling XAS of O_3, with several methods[30] appearing to significantly underestimate the contribution of the 1s(O_C)→ π^* component to the high-energy peak maximum and overestimate the 1s(O_T)→ σ^* contribution. A comparison of the ROKS excitation energies and oscillator strengths at the equilibrium geometry with previously reported results is provided in Table 1, which reveals that most methods considerably overestimate the 1s(O_T)→ σ^* oscillator strength relative to ROKS. The better agreement of ROKS/SCAN with experiment suggests this approach is likely closer to the mark than many wavefunction methods. Nonetheless, it is possible that 1s(O_T)→ σ^* intensity is being underestimated by ROKS/SCAN to some extent, due to the somewhat more rapid decay in the high energy shoulder of the computational high-energy peak as compared to experiment. It seems reasonable to believe that the actual 1s(O_T)→ σ^* transition intensity is bounded from below by ROKS/SCAN and from above by EOM-CC3.

General Behavior of Low Lying Core-Excitations in Biradicals

The reasonably good performance of ROKS in predicting the experimental XAS of O_3 is somewhat surprising, considering the purported multireference character of the molecule. Computation of XAS involves modeling three quantities: the ground state energy, the excited state energy and the transition dipole. For linear-response methods, the excited state model is intrinsically tied to the ground state approximation, and inadequacies in the latter can lead to significant errors in the former (as the correlation free CIS method demonstrates in Fig. 2). For state-specific methods like OO-DFT however, the excited state modeling is decoupled from the ground state and can potentially be done accurately even if the ground state has challenging electronic structure. Indeed, there is no particular reason to presuppose that multireference character of the ground state transfers to the excited state. For core-level excitations of biradicals in particular, transitions to the LUNO analogue result in states representable by a minimal, spin-adapted configuration state function of two determinants. This can be shown by a minimal three-level model involving a core level $|\mathrm{C}\rangle$, and biradicaloid levels $|\mathrm{H}\rangle$ and $|\mathrm{L}\rangle$ (for HONO and LUNO, respectively).

The ground state of the system within this minimal model is $\cos\theta\left|\mathrm{C}^2\mathrm{H}^2\mathrm{L}^0\right\rangle + \sin\theta\left|\mathrm{C}^2\mathrm{H}^0\mathrm{L}^2\right\rangle$, where $0 < \theta < \frac{\pi}{2}$. This leads to a HONO population of $2\cos^2\theta$ and LUNO population of $2\sin^2\theta$. Before accounting for orbital relaxation, the singly core-level excited singlet states can be represented as linear combinations of the CSFs $\frac{1}{\sqrt{2}}\left(\left|\mathrm{C}^{\uparrow}\mathrm{H}^2\mathrm{L}^{\downarrow}\right\rangle + \left|\mathrm{C}^{\downarrow}\mathrm{H}^2\mathrm{L}^{\downarrow}\right\rangle\right)$ and $\frac{1}{\sqrt{2}}\left(\left|\mathrm{C}^{\uparrow}\mathrm{H}^{\downarrow}\mathrm{L}^2\right\rangle + \left|\mathrm{C}^{\downarrow}\mathrm{H}^{\downarrow}\mathrm{L}^2\right\rangle\right)$. However:

$$\cos\theta'\left|\mathrm{C}^{\uparrow}\mathrm{H}^2\mathrm{L}^{\downarrow}\right\rangle + \sin\theta'\left|\mathrm{C}^{\uparrow}\mathrm{H}^{\downarrow}\mathrm{L}^2\right\rangle = -\left|\mathrm{C}^{\uparrow}(\mathrm{H}')^2(\mathrm{L}')^{\downarrow}\right\rangle \qquad (1)$$

where $|\mathrm{H}'\rangle = \cos\theta'|\mathrm{H}\rangle - \sin\theta'|\mathrm{L}\rangle$ and $|\mathrm{L}\rangle' = \cos\theta'|\mathrm{L}\rangle + \sin\theta'|\mathrm{H}\rangle$ (proof provided in supporting information). Therefore, the core to LUNO (or HONO) excitations lead to states that are representable by minimal CSFs of the form $\frac{1}{\sqrt{2}}\left(\left|\mathrm{C}^{\uparrow}(\mathrm{H}')^2(\mathrm{L}')^{\downarrow}\right\rangle + \left|\mathrm{C}^{\downarrow}(\mathrm{H}')^2(\mathrm{L}')^{\uparrow}\right\rangle\right)$. This simplification largely stems from the core-level being energetically isolated from other levels, precluding fractional occupation of this level and any resulting multireference character. It is worth noting that localized core-orbitals interact very weakly with each other, and so there is no reason to consider the effect of more than one core-hole site at a time. This remains true even in highly symmetric systems where delocalized symmetry-adapted linear-combinations of core-orbitals at the formal equilibrium geometry are trivially localized onto individual atoms by vibronic effects.

State-specific CASSCF calculations within this minimal 3 orbital model (consisting of the relevant core-level, HONO and LUNO) numerically confirm Eq. 1 for the lowest excited state wavefunctions arising from O K-edge excitation of ozone. The use of ground state orbitals and energies prevent linear-response methods from taking advantage of the single CSF form of the excited state wavefunction, but state-specific OO in ROKS permits it to model such CSFs properly. We note that the single CSF representability of the lowest core-excited states of pure biradicals (completely unpaired electrons) has been noted in Ref 16. The ground state energy poses less of a challenge, as any empirical alignment of spectra should eliminate most systematic error therein. Even if OO-DFT is utilized without shifting, the ~ 0.3 eV $\equiv 7$ kcal/mol error permissible for excitation energy modeling indirectly allows for some tolerance with regards to correlation missed by a single-reference approximation. This is not the case for modeling ground state thermochemistry where significantly greater accuracy is desired[24].

The transition dipole between a multireference ground state and a single CSF ROKS excited state is less straightforward to model with a single-reference approximation. It appears that the closed-shell RKS approximation to the ground state was sufficient for O_3, but this may not hold for more significantly biradical species with HONO occupations ~ 1.5 (or LUNO ~ 0.5). Very precise spectral intensity predictions for strongly biradical species therefore may be difficult for OO-DFT, but the relative peak positions ought to be effectively modeled to help guide interpretation of experiment. We do however note that single KS determinant based approximations to K-edge oscillator strengths have been found to be reasonably effective in systems with strong electron correlation like transition metal oxides[63,64], indicating that that OO-DFT spectral intensities may be sufficient for many practical applications.

In this regard, it is worth noting that it could be important to consider the doubly excited configurations $\left|C^{\uparrow}(H')^{\downarrow}(L')^{2}\right\rangle$ (i.e. excitations out of a core-level to the fractionally unoccupied HONO analog) in more strongly biradical cases, although these configurations do not appear to be relevant for O_3. ROKS/SCAN estimates the lowest energy state of this nature to be ~ 2.3 eV higher in energy relative to the first spectral peak but with vanishing oscillator strength, which is consistent with the lack of any experimental features in this regime. In nearly pure diradical cases (i.e. HONO and LUNO occupations ~ 1), a fully open-shell ROKS solution for the ground state ought to be a better approximation than RKS. This has been attempted for TR-XAS of singlet excited states in one system[65], but more investigation is required to characterize utility.

We note that while transitions out of the core to frontier orbitals lead to states straightforwardly representable by single CSFs, this does not generalize to excitations to higher energy levels. Such factors may in fact slightly limit ROKS for the $1s(O_T)\rightarrow \sigma^*$ transition of O_3. Nonetheless, it is worth noting that the core-hole formation is likely to dramatically alter the mean-field potential experienced by all the orbitals, and thereby break the near degeneracy between the HOMO and LUMO that leads to biradical character. Consequently, higher energy core-level excitations in biradicaloids may also be quite amenable to modeling with ROKS.

Conclusion

To summarize, we examined the ability of nominally single-reference methods like TDDFT, EOM-CCSD and OO-DFT to reproduce the experimental XAS of O_3, a prototypical biradicaloid. The spectra were computed by treating the molecule like a standard closed-shell species, and vibrational sampling of 128 geometries from the ground state vibrational wavefunction. OO-DFT was found to yield spectra in semiquantitative agreement with experiment when the SCAN functional was used (reasonable results also being obtained from other functionals, as shown in the supporting information). On the other hand, EOM-CCSD and TDDFT bifurcated the experimental high-energy peak into two separate features. Decomposition of computed spectra into excitations from O 1s orbitals to π^* and σ^* levels showed the latter to be significantly broader, indicating the importance of geometry sampling for comparison to experiment over utilizing uniform broadening on results from a single equilibrium structure when excitations to σ^* levels are relevant. For O_3 in particular, the relative intensity of the σ^* excitation at the FC geometry was quite sensitive to the choice of electronic structure method, although broadening through vibrational sampling reduced the differences between different methods somewhat.

We further found that low lying core-level excited states in biradicaloid species (i.e. excitations to the frontier orbitals) are formally representable by single CSFs and are therefore accessible with ROKS. As such, the challenge in modeling XAS of biradicaloids arises from the ground state itself, but this can be mostly mitigated in practice with a purely closed-shell or purely open-shell model, based on HONO/LUNO occupations. Strongly fractional occupation (HONO ~ 1.5, LUNO ~ 0.5) is still expected to pose challenges for OO-DFT methods for oscillator strength predictions, in particular. It would therefore be interesting to have experimental data for biradical species with similar occupations, as they would be useful for stress-testing theoretical methods and highlight where truly multireference approaches would be more important. A potential candidate is para-benzyne, where HONO occupation of $\sim 1.3 - 1.4$ has been estimated[66,67] and a computational XAS prediction has already been made[68]. For less fractional natural orbital occupations, we anticipate that ROKS with reasonable functionals like SCAN would prove adequate, similar to what has been observed for closed-shell species[12].

Computational methods

CIS, TDDFT, CCSD, CCSD(T)[69] and ROKS calculations were performed with Q-Chem 5.4[60], CASSCF calculations with TeraChem[70–72], and CC3 with eT[61]. The EOM-CCSD calculations utilize the frozen-core core-valence separation (fc-CVS) scheme of Ref 9 (as implemented in Q-Chem) to access core-excited states, yielding virtually identical results as an earlier projection based CVS scheme[73] that is implemented in eT (see supporting information). The CIS/TDDFT calculations utilize a reduced single excitation space approach[74] to obtain core-excited states, which only affects excitation energies by $\sim$ 0.01 eV (compared to results utilizing the full single excitation space). We note that the use of TDA instead of full TDDFT using the random phase approximation (RPA) has no impact on the spectrum, as shown in the supporting information.

The FC geometry was optimized using CCSD(T)/aug-cc-pVTZ (1s core held frozen). The ground state vibrational wavefunction was modeled with the harmonic approximation within the same level of theory, and 128 geometries were sampled from it for XAS calculations. No finite temperature or explicit anharmonic effects were included. The CIS, TDDFT, EOM-CCSD, and EOM-CC3 calculations were performed with the aug-cc-pCVTZ basis[19,57,58], while ROKS was performed with the aug-pcX-2[59] basis well-suited for core-hole OO-DFT calculations. The spin-free one-electron X2C relativistic Hamiltonian was used for ROKS calculations[75,76] but not in other cases, due to the large empirical shifts always being necessary for those methods. X2C blueshifts single O(1s) core-hole state energies by 0.3-0.4 eV relative to nonrelativistic results[75].

Acknowledgments

D.H. thanks Dr. Eirik Kjønstad for assistance with the eT program. This research was supported by the AMOS program within the U.S. Department of Energy, Office of Science, Basic Energy Sciences, Chemical Sciences, Geosciences, and Biosciences Division. D.H. was supported by a Stanford Science Fellowship. This work used computational resources of the National Energy Research Scientific Computing Center (NERSC), a U.S. Department of Energy Office of Science User Facility located at Lawrence Berkeley National Laboratory, operated under Contract No. DE-AC02-05CH11231 using NERSC award BES-ERCAP0024588.

Data Availability

The data that supports the findings of this study are available within the article and its supplementary material.

Supporting Information

PDF: Additional computed spectra (TDDFT, ROKS, EOM-CCSD from eT), proof of single CSF nature of excited state wavefunctions.

ZIP: Geometries utilized for the calculations.

Conflicts of Interest

T.J.M. is a co-founder of PetaChem, LLC.

TOC Figure

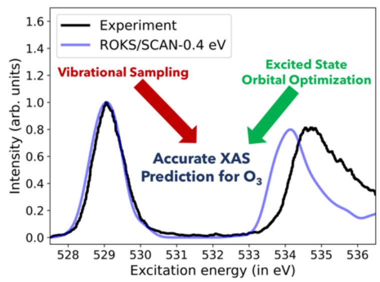

Experiment
ROKS/SCAN-0.4 eV
Vibrational Sampling
Excited State
Orbital Optimization
Accurate XAS
Prediction for O_3
Intensity (arb. units)
Excitation energy (in eV)

References

(1) Stöhr, J. *NEXAFS Spectroscopy*; Springer Science & Business Media, 2013; Vol. 25.

(2) Solomon, E. I.; Hedman, B.; Hodgson, K. O.; Dey, A.; Szilagyi, R. K. Ligand K-Edge X-Ray Absorption Spectroscopy: Covalency of Ligand–Metal Bonds. *Coord. Chem. Rev.* **2005**, *249* (1-2), 97–129.

(3) Kraus, P. M.; Zürch, M.; Cushing, S. K.; Neumark, D. M.; Leone, S. R. The Ultrafast X-Ray Spectroscopic Revolution in Chemical Dynamics. *Nat. Rev. Chem.* **2018**, *2* (6), 82–94.

(4) Bressler, C.; Chergui, M. Ultrafast X-Ray Absorption Spectroscopy. *Chem. Rev.* **2004**, *104* (4), 1781–1812.

(5) Besley, N. A.; Asmuruf, F. A. Time-Dependent Density Functional Theory Calculations of the Spectroscopy of Core Electrons. *Phys. Chem. Chem. Phys.* **2010**, *12* (38), 12024–12039.

(6) Besley, N. A. Modeling of the Spectroscopy of Core Electrons with Density Functional Theory. *Wiley Interdiscip. Rev. Comput. Mol. Sci.* **2021**, *11* (6), e1527.

(7) Hait, D.; Head-Gordon, M. Orbital Optimized Density Functional Theory for Electronic Excited States. *J. Phys. Chem. Lett.* **2021**, *12* (19), 4517–4529.

(8) Wenzel, J.; Wormit, M.; Dreuw, A. Calculating Core-Level Excitations and X-Ray Absorption Spectra of Medium-Sized Closed-Shell Molecules with the Algebraic-Diagrammatic Construction Scheme for the Polarization Propagator. *J. Comput. Chem.* **2014**, *35* (26), 1900–1915.

(9) Vidal, M. L.; Feng, X.; Epifanovsky, E.; Krylov, A. I.; Coriani, S. New and Efficient Equation-of-Motion Coupled-Cluster Framework for Core-Excited and Core-Ionized States. *J. Chem. Theory Comput.* **2019**, *15* (5), 3117–3133.

(10) Peng, B.; Lestrange, P. J.; Goings, J. J.; Caricato, M.; Li, X. Energy-Specific Equation-of-Motion Coupled-Cluster Methods for High-Energy Excited States: Application to K-Edge X-Ray Absorption Spectroscopy. *J. Chem. Theory Comput.* **2015**, *11* (9), 4146–4153.

(11) Paul, A. C.; Myhre, R. H.; Koch, H. New and Efficient Implementation of CC3. *J. Chem. Theory Comput.* **2020**, *17* (1), 117–126.

(12) Hait, D.; Head-Gordon, M. Highly Accurate Prediction of Core Spectra of Molecules at Density Functional Theory Cost: Attaining Sub-Electronvolt Error from a Restricted Open-Shell Kohn–Sham Approach. *J. Phys. Chem. Lett.* **2020**, *11* (3), 775–786.

(13) Bhattacherjee, A.; Schnorr, K.; Oesterling, S.; Yang, Z.; Xue, T.; Vivie-Riedle, R. de; Leone, S. R. Photoinduced Heterocyclic Ring Opening of Furfural: Distinct Open-Chain Product Identification by Ultrafast X-Ray Transient Absorption Spectroscopy. *J. Am. Chem. Soc.* **2018**, *140* (39), 12538–12544.

(14) Pathak, S.; Ibele, L. M.; Boll, R.; Callegari, C.; Demidovich, A.; Erk, B.; Feifel, R.; Forbes, R.; Di Fraia, M.; Giannessi, L.; others. Tracking the Ultraviolet-Induced Photochemistry of Thiophenone During and After Ultrafast Ring Opening. *Nat. Chem.* **2020**, *12* (9), 795–800.

(15) Marchetti, B.; Karsili, T. N.; Kelly, O.; Kapetanopoulos, P.; Ashfold, M. N. Near Ultraviolet Photochemistry of 2-Bromo-and 2-Iodothiophene: Revealing Photoinduced Ring Opening in the Gas Phase? *J. Chem. Phys.* **2015**, *142* (22).

(16) Garner, S. M.; Haugen, E. A.; Leone, S. R.; Neuscamman, E. Spin Coupling Effect on Geometry-Dependent X-Ray Absorption of Diradicals. *arXiv preprint arXiv:2307.15207* **2023**.

(17) Salem, L.; Rowland, C. The Electronic Properties of Diradicals. *Angew. Chemie. Int. Ed.* **1972**, *11* (2), 92–111.

(18) Szabo, A.; Ostlund, N. S. *Modern Quantum Chemistry: Introduction to Advanced Electronic Structure Theory*; Dover Publications, Inc.: Mineola, New York, 1996; pp 286–296.

(19) Dunning Jr, T. H. Gaussian basis sets for use in correlated molecular calculations. I. The atoms boron through neon and hydrogen. *J. Chem. Phys.* **1989**, *90* (2), 1007–1023.

(20) Hayes, E. F.; Siu, A. K. Electronic Structure of the Open Forms of Three-Membered Rings. *J. Am. Chem. Soc.* **1971**, *93* (8), 2090–2091.

(21) Hay, P. J.; Dunning Jr, T. H.; Goddard III, W. A. Configuration Interaction Studies of O_3 and O_3^+. Ground and Excited States. *J. Chem. Phys.* **1975**, *62* (10), 3912–3924.

(22) Miliordos, E.; Xantheas, S. S. On the Bonding Nature of Ozone (O_3) and Its Sulfur-Substituted Analogues SO_2, OS_2, and S_3: Correlation Between Their Biradical Character and Molecular Properties. *J. Am. Chem. Soc.* **2014**, *136* (7), 2808–2817.

(23) Roos, B. O.; Taylor, P. R.; Si, P. E.; others. A Complete Active Space SCF Method (CASSCF) Using a Density Matrix Formulated Super-CI Approach. *Chem. Phys.* **1980**, *48* (2), 157–173.

(24) Karton, A.; Rabinovich, E.; Martin, J. M.; Ruscic, B. W4 Theory for Computational Thermochemistry: In Pursuit of Confident Sub-kJ/Mol Predictions. *J. Chem. Phys.* **2006**, *125* (14).

(25) Rosenqvist, L.; Wiesner, K.; Naves de Brito, A.; Bässler, M.; Feifel, R.; Hjelte, I.; Miron, C.; Wang, H.; Piancastelli, M. N.; Svensson, S.; others. Femtosecond Dissociation of Ozone Studied by the Auger Doppler Effect. *J. Chem. Phys.* **2001**, *115* (8), 3614–3620.

(26) Stranges, S.; Alagia, M.; Fronzoni, G.; Decleva, P. High-Resolution Inner-Shell Photoabsorption and Dissociation of Ozone. *J. Phys. Chem. A* **2001**, *105* (13), 3400–3406.

(27) Helmich-Paris, B. Simulating X-Ray Absorption Spectra with Complete Active Space Self-Consistent Field Linear Response Methods. *Int. J. Quant. Chem.* **2021**, *121* (3), e26559.

(28) Tenorio, B. N. C.; Møller, K. B.; Decleva, P.; Coriani, S. Disentangling the Resonant Auger Spectra of Ozone: Overlapping Core-Hole States and Core-Excited State Dynamics. *Phys. Chem. Chem. Phys.* **2022**, *24* (46), 28150–28163.

(29) Huang, M.; Evangelista, F. A. A Study of Core-Excited States of Organic Molecules Computed with the Generalized Active Space Driven Similarity Renormalization Group. *J. Chem. Phys.* **2023**, *158* (12).

(30) Mazin, I. M.; Sokolov, A. Yu. Core-Excited States and X-Ray Absorption Spectra from Multireference Algebraic Diagrammatic Construction Theory. *J. Chem. Theory Comput.* **2023**, *19* (15), 4991–5006.

(31) Stanton, J. F.; Bartlett, R. J. The Equation of Motion Coupled-Cluster Method. A Systematic Biorthogonal Approach to Molecular Excitation Energies, Transition Probabilities, and Excited State Properties. *J. Chem. Phys.* **1993**, *98* (9), 7029–7039.

(32) Schinke, R. *Photodissociation Dynamics: Spectroscopy and Fragmentation of Small Polyatomic Molecules*; Cambridge University Press, 1995.

(33) Tully, J. C. Molecular Dynamics with Electronic Transitions. *J. Chem. Phys.* **1990**, *93* (2), 1061–1071.

(34) Ben-Nun, M.; Quenneville, J.; Martínez, T. J. Ab Initio Multiple Spawning: Photochemistry from First Principles Quantum Molecular Dynamics. *J. Phys. Chem. A* **2000**, *104* (22), 5161–5175.

(35) Wigner, E. On the Quantum Correction for Thermodynamic Equilibrium. *Phys. Rev.* **1932**, *40* (5), 749.

(36) Zinchenko, K. S.; Ardana-Lamas, F.; Seidu, I.; Neville, S. P.; Veen, J. van der; Lanfaloni, V. U.; Schuurman, M. S.; Wörner, H. J. Sub-7-Femtosecond Conical-Intersection Dynamics Probed at the Carbon K-Edge. *Science* **2021**, *371* (6528), 489–494.

(37) Ridente, E.; Hait, D.; Haugen, E. A.; Ross, A. D.; Neumark, D. M.; Head-Gordon, M.; Leone, S. R. Femtosecond Symmetry Breaking and Coherent Relaxation of Methane Cations via X-Ray Spectroscopy. *Science* **2023**, *380* (6646), 713–717.

(38) Kohn, W.; Sham, L. J. Self-consistent equations including exchange and correlation effects. *Phys. Rev.* **1965**, *140* (4A), A1133.

(39) Frank, I.; Hutter, J.; Marx, D.; Parrinello, M. Molecular Dynamics in Low-Spin Excited States. *J. Chem. Phys.* **1998**, *108* (10), 4060–4069.

(40) Ziegler, T.; Rauk, A.; Baerends, E. J. On the Calculation of Multiplet Energies by the Hartree-Fock-Slater Method. *Theor. Chim. Acta.* **1977**, *43* (3), 261–271.

(41) Thom, A. J.; Head-Gordon, M. Hartree–Fock Solutions as a Quasidiabatic Basis for Nonorthogonal Configuration Interaction. *J. Chem. Phys.* **2009**, *131* (12), 124113.

(42) Kowalczyk, T.; Tsuchimochi, T.; Chen, P.-T.; Top, L.; Van Voorhis, T. Excitation Energies and Stokes Shifts from a Restricted Open-Shell Kohn-Sham Approach. *J. Chem. Phys.* **2013**, *138* (16), 164101.

(43) Foresman, J. B.; Head-Gordon, M.; Pople, J. A.; Frisch, M. J. Toward a Systematic Molecular Orbital Theory for Excited States. *J. Phys. Chem.* **1992**, *96* (1), 135–149.

(44) Hirata, S.; Head-Gordon, M. Time-Dependent Density Functional Theory Within the Tamm–Dancoff Approximation. *Chem. Phys. Lett.* **1999**, *314* (3-4), 291–299.

(45) Sun, J.; Ruzsinszky, A.; Perdew, J. P. Strongly Constrained and Appropriately Normed Semilocal Density Functional. *Phys. Rev. Lett.* **2015**, *115*, 036402.

(46) Hait, D.; Haugen, E. A.; Yang, Z.; Oosterbaan, K. J.; Leone, S. R.; Head-Gordon, M. Accurate Prediction of Core-Level Spectra of Radicals at Density Functional Theory Cost via Square Gradient Minimization and Recoupling of Mixed Configurations. *J. Chem. Phys.* **2020**, *153* (13), 134108.

(47) Perdew, J. P.; Burke, K.; Ernzerhof, M. Generalized gradient approximation made simple. *Phys. Rev. Lett.* **1996**, *77* (18), 3865.

(48) Becke, A. D. Density-functional exchange-energy approximation with correct asymptotic behavior. *Phys. Rev. A* **1988**, *38* (6), 3098.

(49) Lee, C.; Yang, W.; Parr, R. G. Development of the Colle-Salvetti correlation-energy formula into a functional of the electron density. *Phys. Rev. B* **1988**, *37* (2), 785.

(50) Adamo, C.; Barone, V. Toward reliable density functional methods without adjustable parameters: The PBE0 model. *J. Chem. Phys.* **1999**, *110* (13), 6158–6170.

(51) Becke, A. D. Density-functional thermochemistry. III. The role of exact exchange. *J. Chem. Phys.* **1993**, *98* (7), 5648–5652.

(52) Franck, J.; Dymond, E. Elementary Processes of Photochemical Reactions. *Trans. Farad. Soc.* **1926**, *21* (February), 536–542.

(53) Condon, E. A Theory of Intensity Distribution in Band Systems. *Phys. Rev.* **1926**, *28* (6), 1182.

(54) Banna, M. S.; Frost, D. C.; McDowell, C. A.; Noodleman, L.; Wallbank, B. A Study of the Core Electron Binding Energies of Ozone by X-Ray Photoelectron Spectroscopy and the Xα Scattered Wave Method. *Chem. Phys. Lett.* **1977**, *49* (2), 213–217.

(55) Ross, A. D.; Hait, D.; Scutelnic, V.; Haugen, E. A.; Ridente, E.; Balkew, M. B.; Neumark, D. M.; Head-Gordon, M.; Leone, S. R. Jahn-Teller Distortion and Dissociation of CCl_4^+ by Transient X-Ray Spectroscopy Simultaneously at the Carbon K-and Chlorine L-Edge. *Chem. Sci.* **2022**, *13* (32), 9310–9320.

(56) Attar, A. R.; Bhattacherjee, A.; Pemmaraju, C.; Schnorr, K.; Closser, K. D.; Prendergast, D.; Leone, S. R. Femtosecond X-Ray Spectroscopy of an Electrocyclic Ring-Opening Reaction. *Science* **2017**, *356* (6333), 54–59.

(57) Kendall, R. A.; Dunning Jr, T. H.; Harrison, R. J. Electron Affinities of the First-Row Atoms Revisited. Systematic Basis Sets and Wave Functions. *J. Chem. Phys.* **1992**, *96* (9), 6796–6806.

(58) Woon, D. E.; Dunning Jr, T. H. Gaussian basis sets for use in correlated molecular calculations. V. Core-valence basis sets for boron through neon. *J. Chem. Phys.* **1995**, *103* (11), 4572–4585.

(59) Ambroise, M. A.; Jensen, F. Probing Basis Set Requirements for Calculating Core Ionization and Core Excitation Spectroscopy by the *Δ* Self-Consistent-Field Approach. *J. Chem. Theory Comput.* **2018**, *15* (1), 325–337.

(60) Epifanovsky, E.; others. Software for the Frontiers of Quantum Chemistry: An Overview of Developments in the q-Chem 5 Package. *J. Chem. Phys.* **2021**, *155* (8), 084801.

(61) Folkestad, S. D.; Kjønstad, E. F.; Myhre, R. H.; Andersen, J. H.; Balbi, A.; Coriani, S.; Giovannini, T.; Goletto, L.; Haugland, T. S.; Hutcheson, A.; others. eT 1.0: An Open Source Electronic Structure Program with Emphasis on Coupled Cluster and Multilevel Methods. *J. Chem. Phys.* **2020**, *152* (18).

(62) Koch, H.; Christiansen, O.; Jørgensen, P.; Sanchez de Merás, A. M.; Helgaker, T. The CC3 Model: An Iterative Coupled Cluster Approach Including Connected Triples. *J. Chem. Phys.* **1997**, *106* (5), 1808–1818.

(63) Liang, Y.; Vinson, J.; Pemmaraju, S.; Drisdell, W. S.; Shirley, E. L.; Prendergast, D. Accurate X-Ray Spectral Predictions: An Advanced Self-Consistent-Field Approach Inspired by Many-Body Perturbation Theory. *Phys. Rev. Lett.* **2017**, *118* (9), 096402.

(64) Roychoudhury, S.; Prendergast, D. Efficient Core-Excited State Orbital Perspective on Calculating X-Ray Absorption Transitions in Determinant Framework. *Phys. Rev. B* **2023**, *107* (3), 035146.

(65) Haugen, E. A.; Hait, D.; Scutelnic, V.; Xue, T.; Head-Gordon, M.; Leone, S. R. Ultrafast X-Ray Spectroscopy of Intersystem Crossing in Hexafluoroacetylacetone: Chromophore Photophysics and Spectral Changes in the Face of Electron-Withdrawing Groups. *J. Phys. Chem. A* **2023**, *127* (3), 634–644.

(66) Crawford, T. D.; Kraka, E.; Stanton, J. F.; Cremer, D. Problematic p-Benzyne: Orbital Instabilities, Biradical Character, and Broken Symmetry. *J. Chem. Phys.* **2001**, *114* (24), 10638–10650.

(67) Shee, J.; Loipersberger, M.; Hait, D.; Lee, J.; Head-Gordon, M. Revealing the Nature of Electron Correlation in Transition Metal Complexes with Symmetry Breaking and Chemical Intuition. *J. Chem. Phys.* **2021**, *154* (19).

(68) Marin, K.; Huang, M.; Evangelista, F. A. Signatures of Diradicals in X-Ray Absorption Spectroscopy. *J. Chem. Phys.* **2023**, *158* (15).

(69) Raghavachari, K.; Trucks, G. W.; Pople, J. A.; Head-Gordon, M. A fifth-order perturbation comparison of electron correlation theories. *Chem. Phys. Lett.* **1989**, *157* (6), 479–483.

(70) Ufimtsev, I. S.; Martinez, T. J. Quantum Chemistry on Graphical Processing Units. 1. Strategies for Two-Electron Integral Evaluation. *J. Chem. Theory Comput.* **2008**, *4* (2), 222–231.

(71) Ufimtsev, I. S.; Martinez, T. J. Quantum Chemistry on Graphical Processing Units. 2. Direct Self-Consistent-Field Implementation. *J. Chem. Theory Comput.* **2009**, *5* (4), 1004–1015.

(72) Ufimtsev, I. S.; Martinez, T. J. Quantum Chemistry on Graphical Processing Units. 3. Analytical Energy Gradients, Geometry Optimization, and First Principles Molecular Dynamics. *J. Chem. Theory Comput.* **2009**, *5* (10), 2619–2628.

(73) Coriani, S.; Koch, H. Communication: X-Ray Absorption Spectra and Core-Ionization Potentials Within a Core-Valence Separated Coupled Cluster Framework. *J. Chem. Phys.* **2015**, *143* (18).

(74) Asmuruf, F. A.; Besley, N. A. Time Dependent Density Functional Theory Study of the Near-Edge x-Ray Absorption Fine Structure of Benzene in Gas Phase and on Metal Surfaces. *J. Chem. Phys.* **2008**, *129* (6).

(75) Cunha, L. A.; Hait, D.; Kang, R.; Mao, Y.; Head-Gordon, M. Relativistic Orbital-Optimized Density Functional Theory for Accurate Core-Level Spectroscopy. *J. Phys. Chem. Letters* **2022**, *13*, 3438–3449.

(76) Saue, T. Relativistic Hamiltonians for Chemistry: A Primer. *Chem. Phys. Chem.* **2011**, *12* (17), 3077–3094.